Electronic supplementary Material (ESI) for New Journal of Chemistry

Regulable Pyrrolic-N-doped Carbon Materials as an Efficient Electrocatalyst for Selective O_2 Reduction to H_2O_2

Yunxian Zhang,[a] Yongyu Pang,[b] Dong Xia,[b] and Guoliang Chai[b, c]*

[a]*College of Chemistry and Materials Science, Fujian Normal University, Fuzhou, Fujian 350007, P. R. China.*

[b]*State Key Laboratory of Structural Chemistry, Fujian Institute of Research on the Structure of Matter, Chinese Academy of Sciences, Fuzhou 350002, P. R. China. E-mail: g.chai@fjirsm.ac.cn*

[c]*Fujian Science & Technology Innovation Laboratory for Optoelectronic Information of China, Fuzhou, Fujian 350108, P. R. China.*

Corresponding Author
E-mail: g.chai@fjirsm.ac.cn

Electrochemical test for ORR

For all electrochemical measurements, an electrochemical workstation (Autolab PGSTAT302N) is used. Three-electrode system was utilized in the electrochemical measurement in which a glassy-carbon electrode (disk area: 0.196 cm^2) with a Pt ring (ring area: 0.07 cm^2) was used as the working electrode, saturated Ag/AgCl electrode was used as the reference electrode, and a Pt sheet was used as the counter electrode. 4.5 mg of the collected catalyst was dispersed in a mixture of 500 μL of DI water, 40 μL of 5 wt% Nafion solution and 460 μL of isopropanol. After sonication for at least 30 min, 12 μL of the ink was dropped onto the glassy-carbon disk electrode and dried at room temperature. Electrochemical tests were carried out in a 0.1 M KOH electrolyte (pH=13). The electrolytic cell containing the O_2-saturated electrolyte was prepared before electrochemical testing. Oxygen was continuously flowing into the electrolyte during the test. The ring electrode was kept at 1.2 V vs. RHE, which can be used to oxidize the H_2O_2 generated on the disk electrode. The cyclic voltammetry (CV) tests of catalysts were performed between 0.2 and 1.2 V vs. RHE at a scan rate of 200 mV s^{-1} for 10 cycles. The ORR activities were assessed by linear sweep voltammetry (LSV) from 0.2 to 1.2 V vs. RHE at a scan rate of 20 mV s^{-1} and a rotation speed of 1600 rpm. During the LSV, the Pt ring electrode was set at a constant potential of 1.2 V vs. RHE. The CV and LSV curves in N_2-saturated electrolytes were also collected as a reference, respectively. The ring electrode collection efficiency (N) was 0.249 after calibration.

During $2e^-$ ORR, the electron transfer number was calculated from the ring current and disk current as the following equation:

$$n = \frac{4 \times |I_{disk}|}{|I_{disk}| + I_{ring} / N} \tag{1}$$

The H_2O_2 selectivity of $2e^-$ ORR was calculated using the following relation:

$$H_2O_2\% = \frac{200 \times I_{ring}}{|I_{disk}| \times N + I_{ring}} \tag{2}$$

Tafel plots of catalysts were evaluated from the LSV curves. The diffusion-corrected kinetic current density (J_k) was calculated from the following Koutechy–Levich (K-L) equation:

$$J_K = \frac{J \times J_{\lim}}{J_{\lim} - J} \tag{3}$$

where $J_{\lim}$ is the diffusion-limited current density, J_k is the kinetic current density and J is the measured current density. $J_{\lim}$ was calculated as follows

$$J_{\lim} = 0.2nFC_oD_o^{2/3}\nu^{-1/6}\omega^{1/2} \tag{4}$$

where n is the electron transferred number, ω is the electrode rotation speed (in rpm), D_O is the diffusion coefficient of oxygen (1.9×10^{-5} cm^2 s^{-1}), C_O is the volume concentration of O_2 ($C_O = 1.2 \times 10^{-3}$ mol L^{-1}), F is the Faraday constant (96485 C mol^{-1}), ν is the kinematic viscosity of the solution (0.01 cm^2 s^{-1}). Chronopotentiometry stability test was performed by holding the applied disk electrode potential at 0.45 V vs. RHE while the ring electrode potential was maintained at 1.20 V vs. RHE. The electrochemically active surface area was measured by double layer capacitance method. CV scans were conducted at potential window from -0.05 to 0.05 V vs. Ag/AgCl reference electrode with scan rates of 5, 10, 15, 20 and 25 mV s^{-1}. To evaluate the CV cycling stability of the N-CMC-1:5, accelerated durability testing (ADT) of N-CMC-1:5 was performed by sweeping the potential 2500 times between 0.2 and 1.2 V vs. RHE at a scan rate of 200 mV s^{-1}.

Characterizations

X-ray diffraction (XRD) patterns were collected on Miniflex 600 with a scanning speed of 2° per minute. Scanning electron microscopy (SEM) images were obtained using a JSM6700 instrument (JEOL). The structural morphology and elemental distribution were collected on a transmission electron microscope (TEM, JEOL JEM-2010). The X-ray photoelectron spectroscopy (XPS) spectra were performed on an ESCALAB 250XI instrument. Raman spectroscopy was performed from a LabRAM HR spectrometer using a laser at 532 nm wavelength.

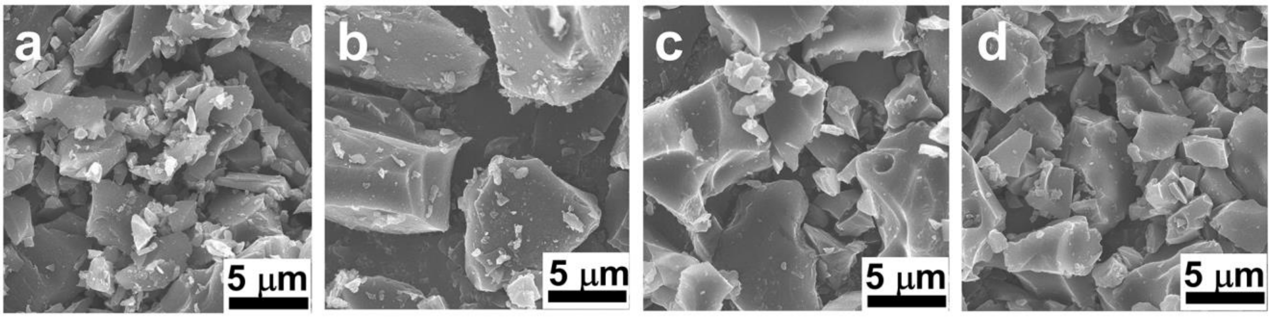

Fig. S1. SEM images of (a) CMC. (b) N-CMC-1:5. (c) N-CMC- 1:1. (d) N-CMC-4:1.

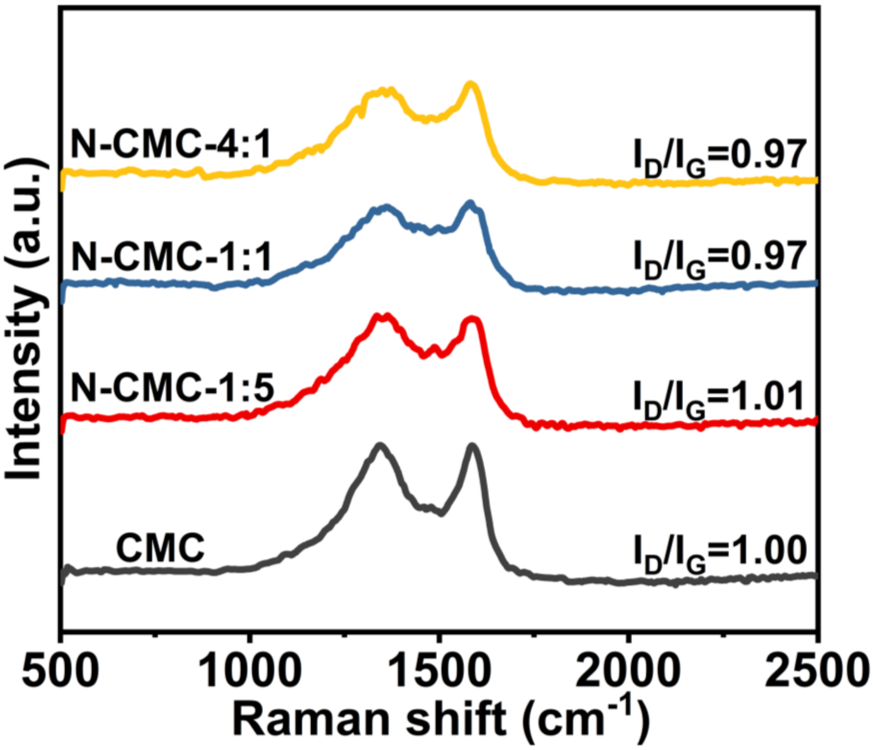

Fig. S2. Raman spectra of CMC, N-CMC-1:5, N-CMC-1:1, and N-CMC-4:1, with I_D/I_G ratios for each sample indicated.

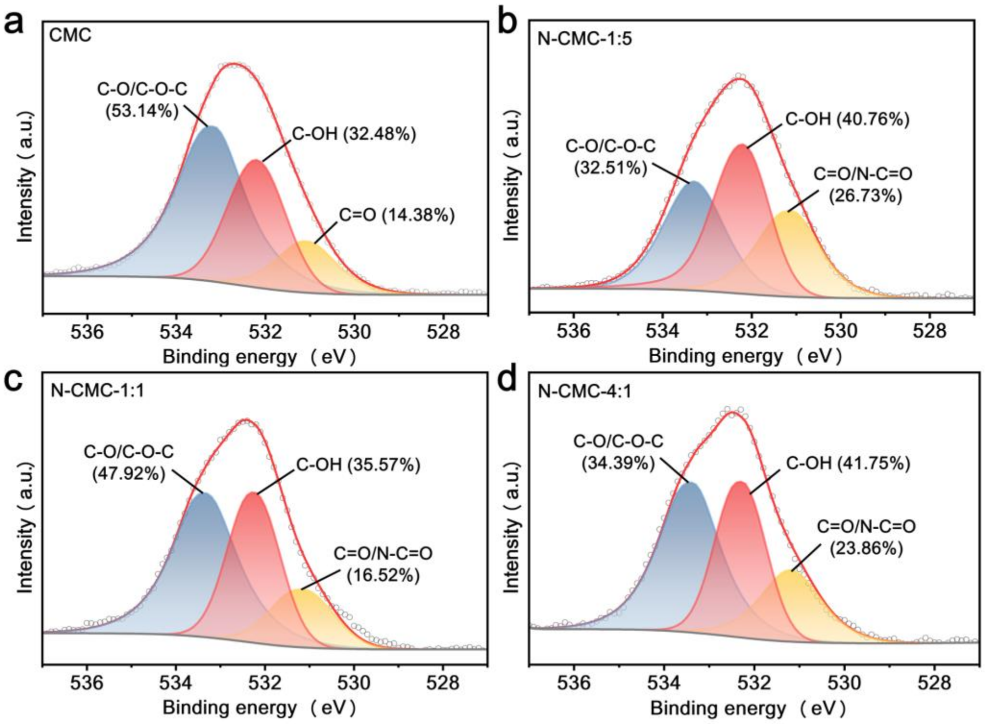

Fig. S3. High-resolution O 1s XPS spectra of (a) CMC, (b) N-CMC-1:5, (c) N-CMC-1:1 and (d) N-CMC-4:1, respectively.

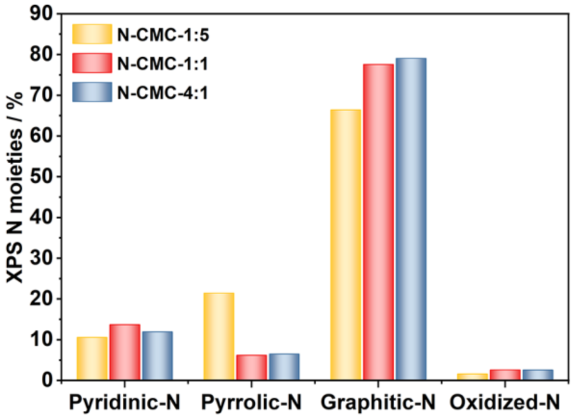

Fig. S4. The relative content change of various nitrogen species of the N-CMCs.

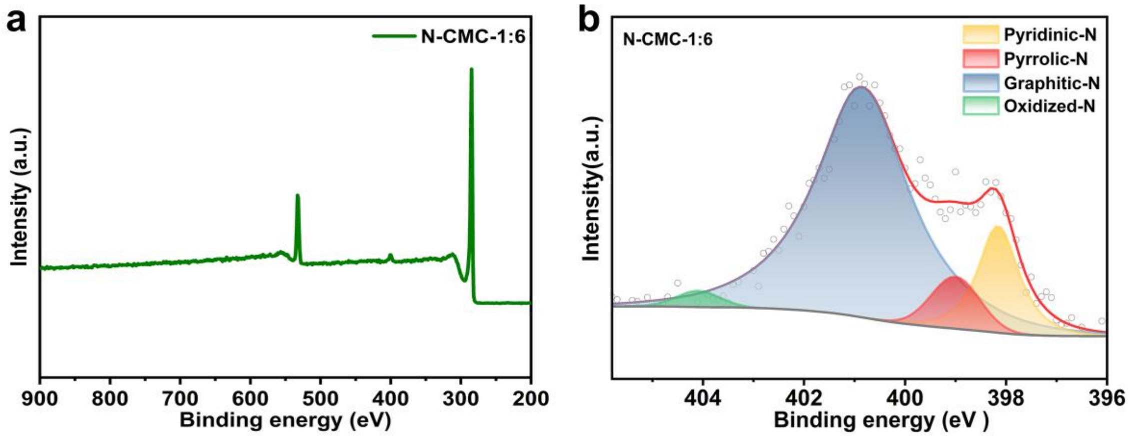

Fig. S5. (a) XPS survey scan of N-CMC-1:6, (b) High-resolution N1s XPS spectrogram of N-CMC-1:6.

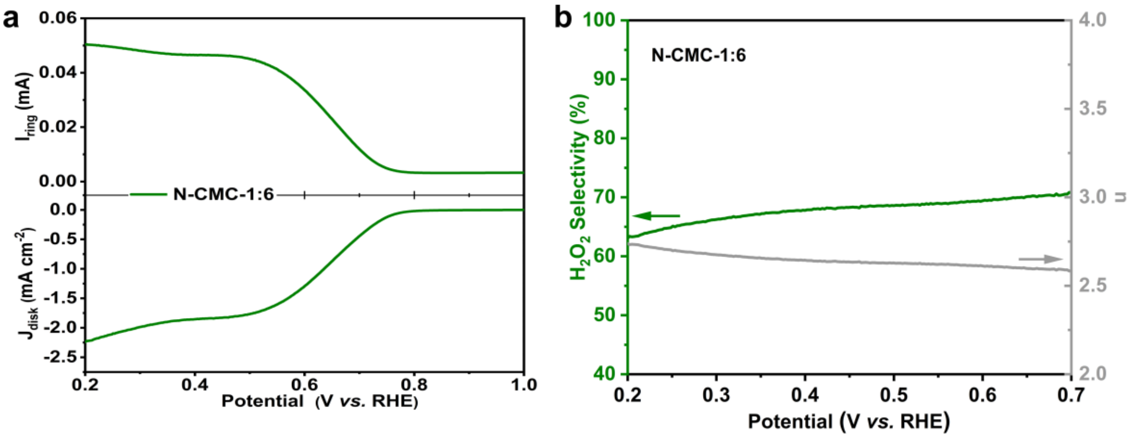

Fig. S6. (a) Linear sweep voltammetry of N-CMC-1:6 with the disk current density, ring current, (b) H_2O_2 selectivity and Electron transfer numbers (n) of N-CMC-1:6.

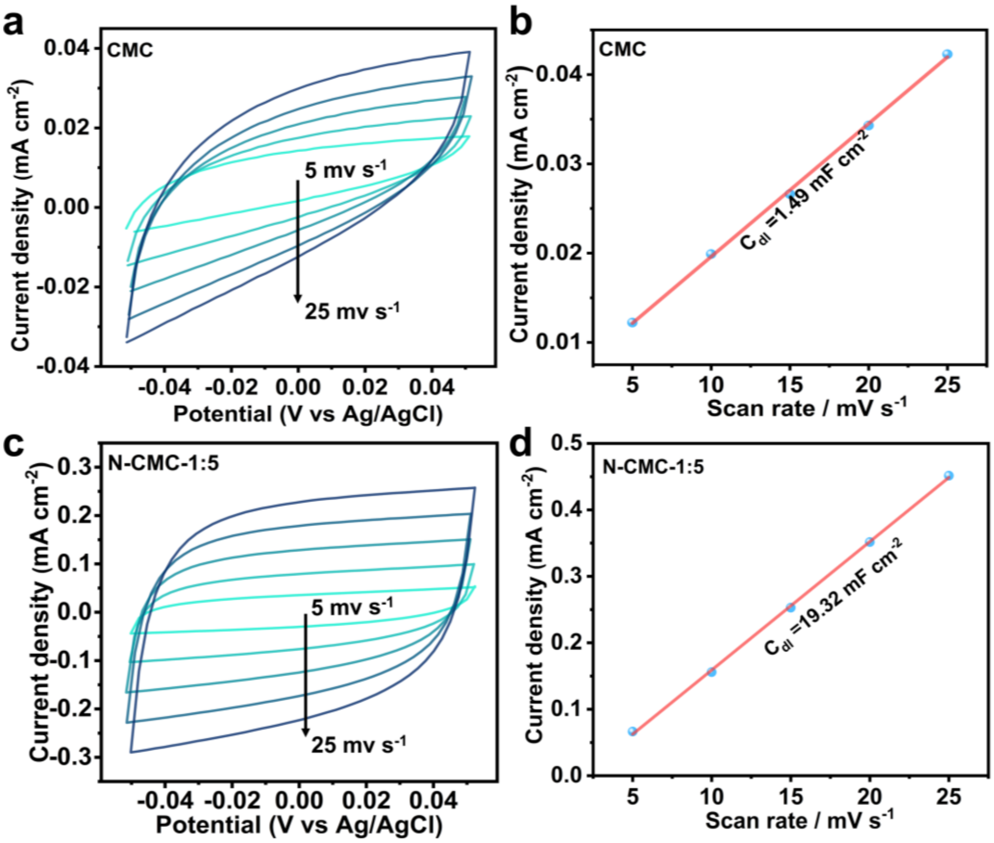

Fig. S7. (a, c) CV for CMC and N-CMC-1:5 modified electrodes in the double layer region at scan rates of 5, 10, 15, 20, and 25 mV s^{-1} in 0.1 M KOH aqueous electrolyte. (b, d) current (taken at the potential of 0 V vs. Ag/AgCl) as a function of scan rate derived from (a, c), respectively.

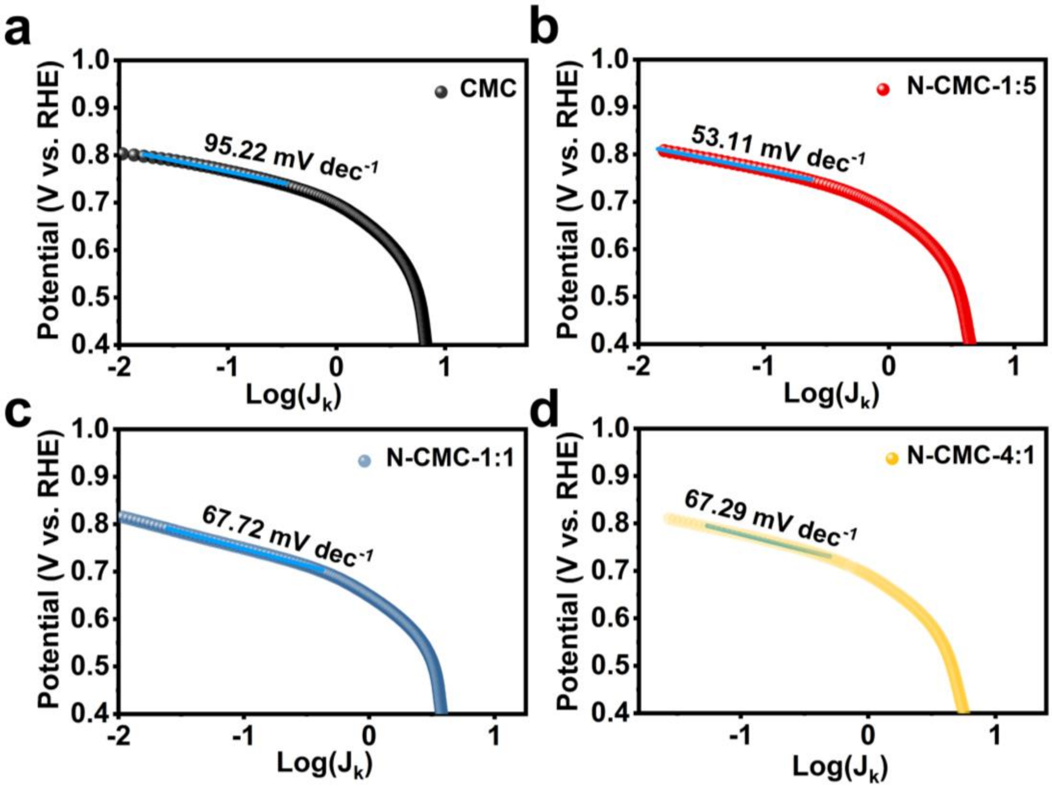

Fig. S8. Tafel plots for CMC, N-CMC-1:5, N-CMC-1:1 and N-CMC-4:1 for ORR in 0.1 M KOH.

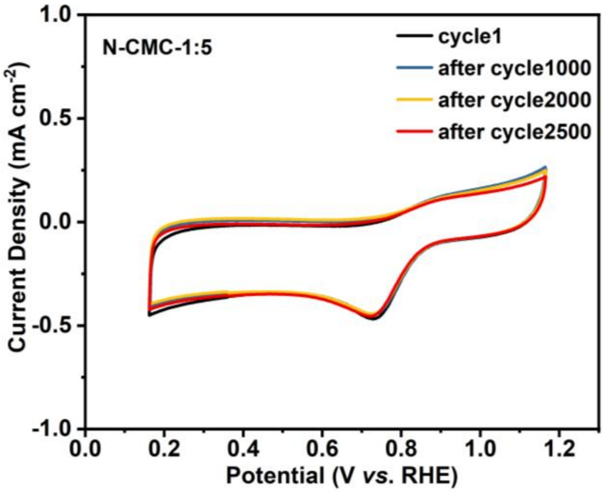

Fig. S9. CV cycling Stability performance of N-CMC-1:5 in 0.1 M KOH.

Table S1. Atomic content of C, O and N for CMC and N-CMCs according to XPS survey spectra.

Sample	C (at.%)	O (at.%)	N (at.%)
CMC	91.15	8.85	0.00
N-CMC-1:6	85.95	11.18	2.87
N-CMC-1:5	83.08	13.77	3.15
N-CMC-1:1	88.70	7.32	3.99
N-CMC-4:1	87.50	8.11	4.39

Table S2. The percentage of different nitrogen configurations for N-CMCs.

Sample	N (at.%)	Pyridinic-N (%)	Pyrrolic-N (%)	Graphitic-N (%)	Oxidized-N (%)
N-CMC-1:6	2.87	14.99	7.53	75.34	2.14
N-CMC-1:5	3.15	10.56	21.43	66.41	1.59
N-CMC-1:1	3.99	13.69	6.18	77.55	2.58
N-CMC-4:1	4.39	11.90	6.46	79.09	2.56

Table S3. Comparison of 2e$^-$ ORR performance for different electrocatalysts.

	pH	Potential (V_{RHE})	Selectivity (%) for 2e$^-$ ORR	References
Co–N–C	13	0.20V	~82%	1
Mesoporous defective carbon	13	0.55V	80%	2
N-CMC-1:5	**13**	**0.42V**	**~81.4%**	**This work**
M_{O1}/OSG-H	13	0.35V	95%	3
NCMK3IL50_800T	7	0.2V	75.7%	4
Hierarchically porous carbon	7	0.16V	70.8%	5
RO-SWCNHs	7	0.30V	95%	6

Reference:

1. B. Q. Li, C. X. Zhao, J. N. Liu and Q. Zhang, *Adv. Mater.*, 2019, **31**, 1808173.
2. S. Chen, Z. Chen, S. Siahrostami, T. R. Kim, D. Nordlund, D. Sokaras, S. Nowak, J. W. F. To, D. Higgins, R. Sinclair, J. K. Norskov, T. F. Jaramillo and Z. Bao, *ACS Sustain. Chem. Eng.*, 2018, **6**, 311-317.
3. C. Tang, Y. Jiao, B. Shi, J.-N. Liu, Z. Xie, X. Chen, Q. Zhang and S.-Z. Qiao, *Angew. Chem. Int. Ed.*, 2020, **59**, 9171-9176.
4. Y. Sun, I. Sinev, W. Ju, A. Bergmann, S. Dresp, S. Kuehl, C. Spoeri, H. Schmies, H. Wang, D. Bernsmeier, B. Paul, R. Schmack, R. Kraehnert, B. Roldan Cuenya and P. Strasser, *ACS Catal.*, 2018, **8**, 2844-2856.
5. Y. Liu, X. Quan, X. Fan, H. Wang and S. Chen, *Angew. Chem. Int. Ed.*, 2015, **54**, 6837-6841.
6. Y. Liu, J. Zhang, S. He, Y. Cui and L. Guan, *J. Energy Chem.*, 2021, **54**, 118-123.